Available online at www.sciencedirect.com
SCIENCE DIRECT
Polymer 47 (2006) 4124–4131
polymer
www.elsevier.com/locate/polymer

Sequestration of electroactive materials in a high T_g, insulating polymer matrix for optoelectronic applications. Part 2. Photovoltaic devices

Xuezhong Jiang, William F. Burgoyne Jr, Lloyd M. Robeson *

Air Products and Chemicals, Inc., 7201 Hamilton Blvd., Allentown, PA 18195, USA

Available online 7 March 2006

Abstract

The incorporation of high levels of electroactive compounds into a high T_g matrix polymer was investigated in photovoltaic (PV) devices. The combination of electron donor–electron acceptor pairs with optionally light harvesting organics (e.g. laser dyes) in the high T_g polymer matrix yielded PV performance in the range of literature data typically reported for organic based PV devices. The advantages for using a high T_g matrix include increasing the T_g of the electroactive compounds, preventing crystallization, improving the mechanical properties of the active layer(s) and the ability to employ lower cost fabrication processes. While the basic concept has been demonstrated, further optimization would be required to achieve a useful combination of photovoltaic properties. As in the companion paper on utilization of a high T_g polymer to sequester low molecular weight electroactive species for LED devices, this paper demonstrates the same concept for PV devices. The approach to solve the issues with low molecular weight electroactive species noted in the literature to date often involves covalent bonding of these compounds to polymeric backbones. This and the companion paper well-illustrates the blend approach is equally viable and offers a much simpler methodology.

Keywords: Photovoltaic devices; High T_g polymer; Optoelectronic applications

1. Introduction

A photovoltaic (PV) device absorbs light and generates electricity. It is virtually the reverse of a light emitting diode (LED) device that emits light upon application of an electric field. Crystalline silicon based PV devices have been used since the 1960s with initial use in space applications followed by utility in remote installations requiring an electrical power source. Further developments have yielded broad utility in various industrial and consumer applications, such as hand-held calculators, telecommunications, signal lights, home electrical generation, as well as grid-connected power generation [1]. In addition to crystalline silicon, other inorganic based semiconductors composed of amorphous silicon, gallium arsenide, CdS–CdTe, $CuInSe_2$–CdS and CdTe inorganic based semiconductors have been noted to offer promising results for PV applications [1,2]. Organic materials employed in PV devices offer a potentially lower cost alternative to the traditional silicon based devices, such as solar cells and photodetectors. The performance attributes of organic/polymeric based PV devices, however, need significant improvements in efficiencies and lifetime before they can realize the potential demonstrated by inorganic based systems.

The recognition of organic/polymeric semiconductor utility for PV applications emerged soon after the initial discoveries of potential use in light emitting diodes [3–6]. In inorganic based PV devices, the photovoltaic process involves an incident photon exciting an electron from the valence band into the conduction band of a semiconductive material as long as the photon energy is in excess of the semiconductor band gap. In organic semiconductor based PV devices, the absorption of photons in the light harvesting layers create excitons which dissociate into holes and electrons at an interface and move through the respective hole transport and electron transport paths to the electrodes creating current. The interest in organic/polymer based PV devices significantly increased with the observation that electron donor–electron acceptor combinations can yield higher efficiencies.

Compared with LED devices, photovoltaic devices utilize the same or similar materials in the device construction although there are often significant differences in the light harvesting layer versus the light emitting layer of the LED devices. Low molecular weight compounds such as perylenes, pyrromethene dyes, rhodiamine dyes, and coumarin dyes have been noted as light absorbers for PV devices. Conjugated polymers including poly(phenylene vinylenes), polyanilines, and polythiophenes have been evaluated as light harvesting

* Corresponding author. Tel.: +1 610 481 5026; fax: +1 610 706 6586.
E-mail address: robesolm@apci.com (L.M. Robeson).

0032-3861/$ - see front matter © 2006 Elsevier Ltd. All rights reserved.
doi:10.1016/j.polymer.2006.02.035

materials. The concept of donor–acceptor complexes combining hole transport organics (electron donors) with electron transport organics (electron acceptors) has been an important approach for light harvesting materials towards achieving higher device efficiencies. An early report on this approach involved blends of fullerenes (C_{60}) (electron acceptor) with MEH-PPV (electron donor) in which the energy conversion efficiencies were several orders of magnitude better than MEH-PPV alone [7]. Another version of this concept involved conjugated polymer blends comprising an electron donor (MEH-PPV) and an electron acceptor (cyano-PPV), offering one to two orders of magnitude higher energy conversion efficiency than the individual polymers in PV devices [8]. This work provided the basis for the concept of bulk heterojunction morphologies involving phase separated polymers, and the potential for spinodal decomposition to provide co-continuous phase structure for both polymers. This is important as the formation of an exciton followed by dissociation into an electron and hole at the donor–acceptor phase boundary requires a pathway to the respective electrodes in order to extract electrical power from the device. A specific study involving phase separated donor–acceptor polymer combinations for PV devices employed fluorene copolymer blends comprising comonomers with electron donor and electron acceptor groups [9]; the best results were obtained when the morphology was quenched at nanoscale dimensions. Small molecule donor–acceptor combinations have also been used in heterojunction PV devices. Copper phthalocyanine/3,4,5,10-perylene tetracarboxylic bis-benzimidazole (PTCBI) were codeposited, yielding phase separation with nanoscale dimensions [10]. Heterojunction approaches in PV devices have been discussed by Nelson [11] and Brabec et al. [12].

Electroactive polymer blends with low molecular weight electroactive compounds have also been investigated. Perylene tetracarboxylates (electron acceptors) combined with poly(3-hexylthiophene) (P3HT) (electron donor) offered higher efficiency than P3HT alone [13]. Poly(*N*-vinyl carbazole) (PVK) blended with metallo-porphyrins exhibited higher conversion efficiencies than the metallo-porphyrin alone in the same PV device design [14]. The bulk of the investigations of conjugated polymer (electron donor) combinations with low molecular weight electron acceptors, however, involve fullerene based electron acceptors as noted in recent references [15–18]. The incorporation of low molecular weight electroactive organic or organo-metallic materials in insulating polymers for PV applications has had very limited activity. Several early patents and publications employed insulating polymers as binders for organic photoconductors [19–22]. Tang et al. [19] described blends of pyrylium dyes with organic photoconductors such as aromatic tertiary amines and styrylstilbenes in a polycarbonate matrix in a PV device. The spin-coated electroactive layer was exposed to solvent vapor to cause aggregation (phase separation) of the electroactive species. Loutfy et al. [20] described phthalocyanine (metal-free) blends in a polymer matrix employed in PV devices. In this case, the polymer was also used as binder with phthalocyanine phase separated into discrete particles. The use of polymer binders for particulate phthaolocyanine PV devices showed that the best results were obtained with highly polar polymers such as polyacrylonitrile and poly(vinylidene fluoride) [23]. Poly(methyl methacrylate) doped with fluorescent perylene dye was characterized by various techniques for luminescent solar concentrator applications, however, no PV device performance data was reported [24]. In order to employ lower cost fabrication routes, electroactive compounds attached to polymeric backbones have been suggested. Ink-jet printing of solar cell devices was investigated with an electron donor/electron acceptor blend of a pyridyl ruthenium complex attached to poly(methyl methacrylate) and a fullerene derivative [25].

This study is directed at the use of high T_g insulating polymers to sequester high concentrations of hole transport, electron transport and light harvesting species in single light harvesting layer of a PV device. Low molecular weight electroactive compounds often have glass transition temperatures too low for utility as well as the tendency to crystallize. Low molecular weight materials are generally applied by vacuum deposition as the lower cost fabrication routes of spin coating, ink-jet printing and roll-to-roll coating are generally not preferred and often not adequate. The mechanical properties of low molecular weight materials are also not adequate for flexible devices. The addition of a high T_g polymer as a matrix for the low molecular weight electroactive materials can resolve many of these deficiencies. Unlike several references noted above employing polymeric binders where the electroactive species are phase separated [19–21], this study was designed to evaluate single phase insulating polymer/electroactive material compositions. The concept of donor–acceptor pairs in this investigation involved combining hole transport and electron transport materials in the same polymer matrix. This concept has been previously discussed in a conference proceedings [26] as well as a patent application [27]. Specific data and figures from [26] have been included (with permission) in this paper.

A two layer heterojunction material involving a layer of the high T_g polymer with the hole transport material on the anode and another layer with the high T_g polymer with the electron transport material next to the cathode would employ the same basic concept as described in a patent application [27] discussing this concept.

2. Experimental

The polymers chosen to demonstrate the potential of sequestration of low molecular weight electroactive species in a PV device are a poly(aryl ether) (PAE-2) and a polyarylate. PAE-2 is a condensation polymer from 4,4′-dibromobiphenyl and 9,9-bis(4-hydroxyphenyl)fluorene produced by the Ullman reaction [28] offering a high T_g (265 °C), good solvent solubility and miscibility with a wide range of low molecular weight electroactive species. Polyarylate (the condensation polymer of Bisphenol A and tere/*iso* phthalates (PAR)) was chosen based on exceptional UV stability [29] thus relevant for PV applications. The high T_g polymers and key electroactive

species employed in the experimental studies are shown in Fig. 1.

The construction of PV device is very similar to that of OLEDs (organic light emitting diodes) and PLEDs (polymer light emitting diodes). This is not surprising considering that the device structure of OLED and PV devices are essentially the same. The PV device can include a hole extraction layer, a hole transport layer, a light harvesting layer, an electron transport layer, and an electron extraction layer. In most devices only several layers are employed; usually a hole extraction layer (HEL) and light harvesting layer (LHL). The determination of the device performance involves the measurement of the current–voltage (I–V) characteristics with application of an incident light source (such as a xenon lamp or a solar simulator providing a simulated solar spectrum). Generalized I–V curves are shown in Fig. 2(a) and (b) for a PV device under illumination. The key variables for evaluation of the PV device performance are: (1) open circuit voltage V_{oc}, which is the voltage at $I=0$ A; (2) short circuit current I_{sc}, which is the current at $V=0$ V; (3) photocurrent density, which is the photocurrent divided by the device active area; (4) fill factor FF, which is the ratio of maximum power $(IV)_{max}$ to the product of I_{sc} and V_{oc}, i.e. $FF=(IV)_{max}/(I_{sc}V_{oc})$; (5) external quantum efficiency, which is the ratio of the number of charges extracted out of the device to the number of incident photons; (6) internal quantum efficiency, which is the

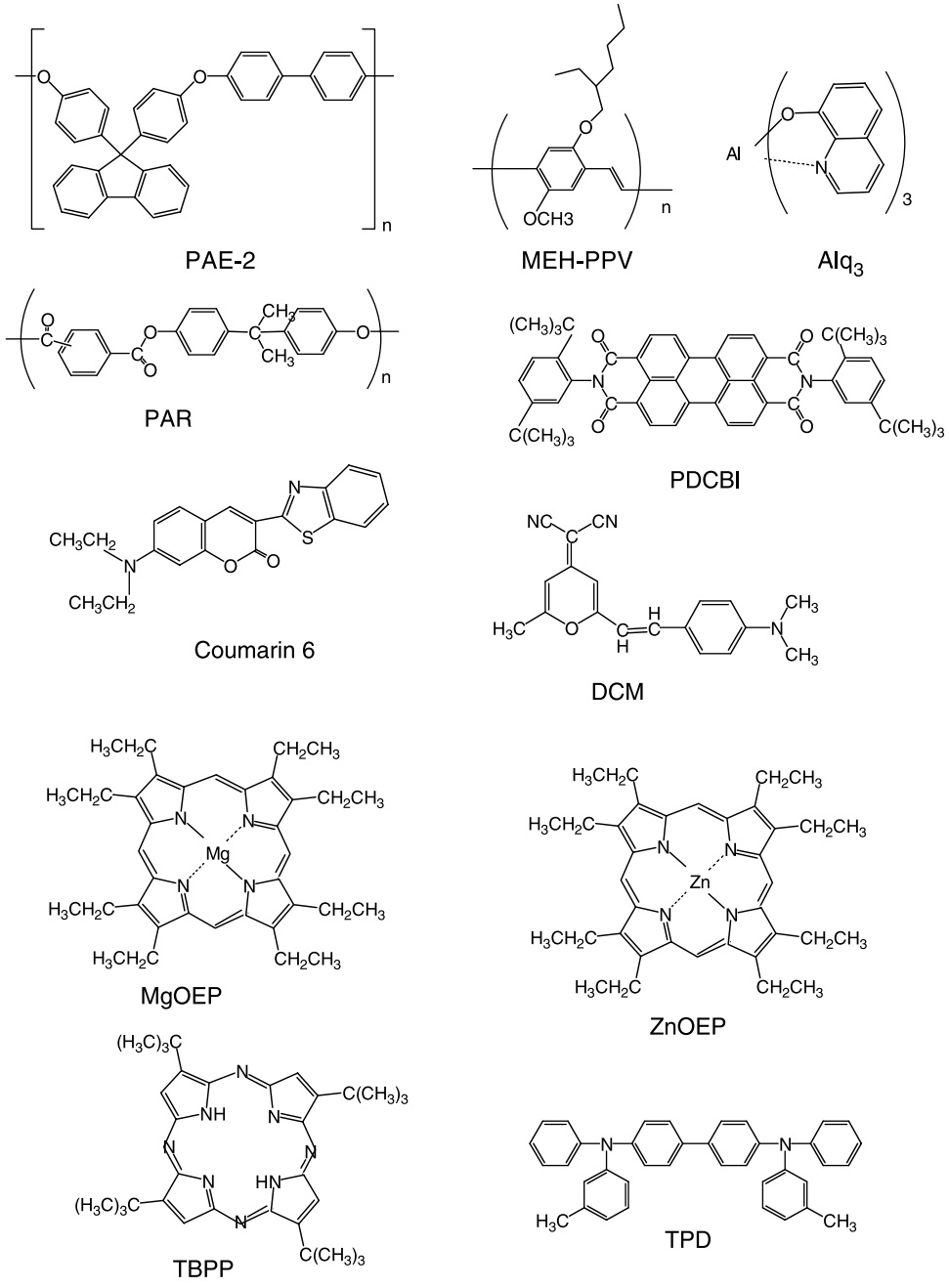

Fig. 1. Chemical structures of the materials used in PV device evaluation.

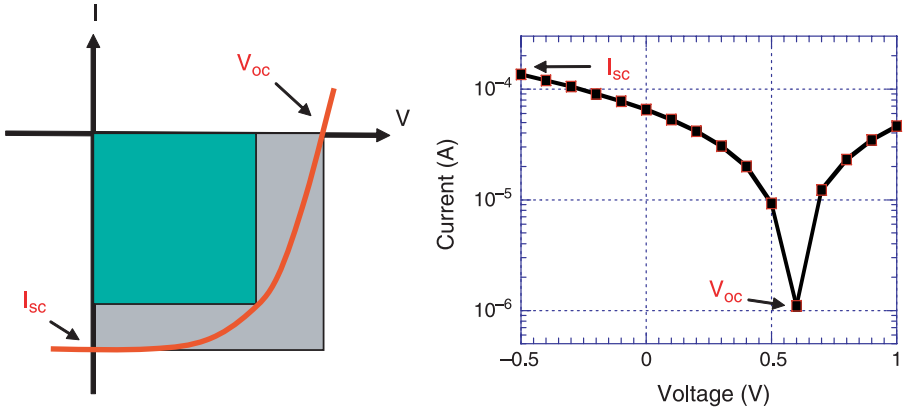

Fig. 2. (a) Current–voltage characteristic of a PV device under illumination; (b) a current–voltage characteristic on a log scale.

ratio of the number of charges extracted out of the device to the number of photons absorbed by the device; (7) power efficiency, which is the value of generated electrical power divided by incident optical power P_{op}, maximum power efficiency is $FF(I_{sc}V_{oc})/P_{op}$.

Photoluminescence (PL) efficiencies were measured using an Oriel InstaSpec IV CCD camera and a Newport integrating sphere from thin films spin-coated on quartz substrates [30]. Output of a 150 W ozone free xenon lamp from Oriel Instruments that was monochromatized by an H10 compact monochromator from Jobin Yvon was used as the excitation light source.

The photovoltaic devices were fabricated on ITO (indium tin oxide) substrates with a sheet resistance of ~12 Ω/□ (from Colorado Coating Concept). The ITO substrates were ultrasonicated sequentially in DI water with detergent, methanol, isopropanol and acetone. The ITO substrates were further cleaned with oxygen plasma in an SPI Desktop II oxygen plasma etcher for 10 min. For the hole extraction layer, Baytron P AI4083 (poly(ethylene-3,4-dioxythiophene):poly(styrene sulfonic acid) (PEDOT:PSSA, from Bayer)) was spin-coated at a spin rate of 3000 rpm from its water dispersion and cured at 160 °C for 30 min under a nitrogen atmosphere. The PEDOT:PSSA dispersion was filtered with a 0.45 μm PVDF filter prior to spin coating. The light harvesting layer containing the high T_g polymer along with the hole transport material, the electron transport material and optionally the light harvesting material was spin-coated from their chlorobenzene solutions with concentration ranging from 10 to 18 mg/mL at spin rates from 1000 to 2000 rpm. The samples were then masked and transferred into the chamber of a vacuum evaporator located inside an argon atmosphere dry box. A layer of 30 nm thick calcium (Ca) or 150 nm Al was vacuum deposited at about 1×10^{-7} Torr through the mask. In the case of Ca, another layer of 120 nm thick silver (Ag) was deposited on top of the Ca layer to lower the electrode resistance and provide protection for the Ca layer. The device testing was promptly carried out in air at room temperature. The thicknesses of the films were determined with a KLA Tencor P15 surface profilometer. Current–voltage characteristics were measured using a Keithley 2400 SourceMeter at a data sampling frequency of 0.1 V. The resolution (precision) of the current measurement was 10 nA. The 150 W ozone free xenon lamp was used as the illuminating light source for the characterization of PV devices. The light was focused onto the devices using a lens. For the characterization of PV devices under monochromatic illumination (action spectrum measurements), the H10 compact monochromator from Jobin Yvon was used with the xenon lamp.

3. Results and discussion

When selecting the hole transporting and electron transporting material pair for PV application, one needs to consider their energy levels. The HOMO (highest occupied molecular orbital) and LUMO (lowest un-occupied molecular orbital) levels of the material pair need to match in such a way that exciton dissociation (charge separation) will be favored at the interface of the two materials. One way to verify charge separation is to measure the PL quantum efficiency of either component in the blend of the two materials. If the PL efficiency of either component in the blend is lower than that of the individual component alone, the exciton is quenched by charge separation.

N,*N*′-Bis(2,5-di-*tert*-butylphenyl)-3,4,9,10-perylenedicarboximide (PDCBI) was used as the electron transporting material for device fabrication because it is soluble in organic solvent such as chlorobenzene. Mixtures of PDCBI with different hole transporting materials in PAE-2 were coated onto quartz substrates for PL efficiency measurement. The hole transporting materials used were DCM, TPD, and MEH-PPV. Films were drop-cast since the weight ratio of the active components (either hole or electron transporting materials or both) was limited to below 20 wt% to avoid the concentration quenching problem. Consequently, a relatively thick film is required to achieve reasonable PL intensity for the efficiency measurement. Such a thick film necessitated drop casting. The film morphology thus obtained might be different than that of a spin-coated film. However, a better charge separation efficiency in spin-coated films than in drop cast films was expected because phase separation at a smaller scale was expected in the spin-coated films. Therefore, the PL quenching

efficiency measured here represents the lower limit of the quenching efficiency of a spin-coated film. Table 1 summarizes the results. The quantum efficiencies of 5.0 wt% DCM in PAE-2, 15 wt% TPD in PAE-2, 6.4 wt% PDCBI in PAE-2, and MEH-PPV pure film are 16–17, 24.1, ~4.5 and 18%, respectively. When DCM and PDCBI were mixed at a weight ratio of 5:8, the efficiency of the resulting film drops to below 1%. The efficiency of the mixtures of TPD:PDCBI (5:2 by weight) and MEH-PPV:PDCBI (5:1 by weight) was not measurable. The photoluminescence was totally quenched, which indicated a very efficient charge separation at the interface of the material pairs. Therefore, each of the combinations demonstrated very efficient charge separation and seems promising for the PV application. The absorption of PDCBI peaks at about 528 nm, which is suitable for PV application.

Fig. 3 shows the HOMO and LUMO energy levels of the hole and electron transporting materials obtained from literature sources [31–34]. The energy level alignment accounts for the observed PL quenching in the case of TPD:PDCBI, DCM:PDCBI and MEH-PPV:PDCBI. The HOMO and LUMO levels of PDCBI were lower than those of TPD, DCM and MEH-PPV, favoring hole transfer from PDCBI to these hole transporting materials, and electron transfer from the hole transporting material to PDCBI. One concern is that the LUMO level of PDCBI was very close to the HOMO levels of TPD, DCM and MEH-PPV, which could possibly result in exciplex formation and compete with PV effect. The exciplex emission will be present in the PL spectrum if indeed the exciplex can be formed. However, it was above 1000 nm and out of our CCD detection range (300–1000 nm).

Initially, a blend of DCM and Alq_3(aluminum tris(8-hydroxyquinoline)) (1:1 by weight) was tested in a PV device structure. DCM and Alq_3 were mixed with PAE-2 (the ratio of DCM + Alq_3 vs. PAE-2 is 4:3 by weight) in chlorobenzene (CB). A double layer device with configuration of ITO/PEDOT/PAE-2:DCM:Alq_3/Mg/Ag was fabricated. However, no PV effect was detected. The relative position of the HOMO and LUMO energy levels of DCM and Alq_3 can shed light on the result. As can be seen from Fig. 3, the HOMO and LUMO levels of DCM actually are located inside those of Alq_3, so not only holes will be transferred from Alq_3 to DCM, electrons will also be transferred from Alq_3 to DCM. The net result was exciton or energy transfer from Alq_3 to DCM. As a result, EL was observed from the device.

Table 1
Photoluminescence quantum efficiency (η_{PL}) of thin films of polymer blends

Composition	$\lambda_{excitation}$ (nm)	η_{PL}
MEH-PPV	365	18.0%
TPD in PAE-2 (15 wt%)	365	24.1%
DCM in PAE-2 (5.0 wt%)	365	17.3%
	500	16.2%
PDCBI in PAE-2 (6.4 wt%)	365	4.6%
	500	4.1%
DCM:PDCBI (5:8) in PAE-2 (10 wt%)	365	0.44%
	500	0.89%
TPD:PDCBI (5:2) in PAE-2 (18 wt%)	365	PL totally quenched
	500	PL totally quenched
MEH-PPV:PDCBI (5:1)	365	PL totally quenched
	500	PL totally quenched

The ratios shown are weight ratios.

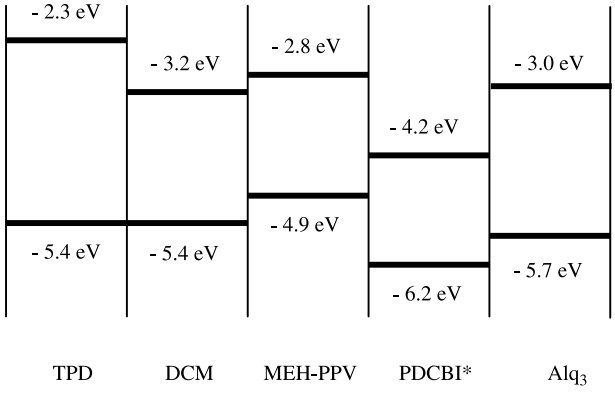

* values listed for similar structure

Fig. 3. Energy diagram of the hole and electron-transporting materials.

Because the blend of TPD:PDCBI showed total PL quenching, PV devices based on TPD:PDCBI with different polymer hosts and cathodes were studied. The host polymers used were PAE-2 and polyarylate (PAR). The photoactive and electroactive species used were TPD, PDCBI, and Coumarin 6 (C6). The device area was about 6.3 mm^2. The performance of the devices is summarized in Table 2. Representative *I–V* characteristics measured from device ITO/PEDOT/PAE-2:TPD:PDCBI:C6 (31:33:25:11)/Al, both in the dark and under illumination, are shown in Fig. 4. Since charge separation at the TPD/PDCBI interface is very efficient, all the devices showed good PV effect. The fill factor of the devices is relatively low, between 0.20 and 0.30. The main reason of the low fill factor is probably the high resistance of the photoactive layer due to the low carrier mobility of the film.

As shown in the energy diagram illustrated in Fig. 3, the HOMO and LUMO levels of TPD and PDCBI are well aligned. Light absorption and exciton generation in either TPD or PDCBI molecule/phase can contribute to the photovoltaic effect (charge carrier generation). One way to study the mechanism and to verify the contribution of the TPD and PDCBI is to measure the action spectrum of the device. The action spectrum measures response of the photocurrent (ideally quantum efficiency) of the device to single wavelength illumination. To obtain the action spectrum, the xenon lamp was monochromatized before it was illuminated on the device. The photocurrent of the device was measured under the single wavelength illumination. Fig. 5 shows the action spectrum of the device. The spectrum had two peaks, one between 300 and 400 nm and the other between 420 and 600 nm. This spectrum agreed with the UV–vis absorption spectrum of the PAR:TPD:PDCBI blend film, which is shown in Fig. 6. The contribution of the first peak was due to absorption by TPD, while the contribution of the second peak was due to absorption

Table 2
Performance of PV devices with a structure of ITO/PEDOT/photoactive layer/cathode

Active layer composition	Cathode	Open circuit voltage V_{oc} (V)	Short circuit current I_{sc} (μA)	Fill factor FF
PAE-2:TPD:PDCBI (28:35:37)	Al	0.60	0.86	0.20
PAE-2:TPD:PDCBI (31:39:30)	Ca	0.80	13.1	0.23
PAE-2:TPD:PDCBI (31:40:29)	Ag	0.60	22.8	0.26
PAR:TPD:PDCBI (37:30:33)	Al	0.80	61.8	0.27
PAE-2:TPD:PDCBI:C6 (31:33:25:11)	Al	0.60	65.0	0.28
PAR:TPD:PDCBI (37:30:33)[a]	Al	0.60	86.2	0.26
PAE-2:TPD:PDCBI (31:33:25)[a]	Al	0.40	33.3	0.30

[a] A film of PAE-2:C6 (9:10) was spin-coated as a light harvesting layer on the other side of the glass substrate after the device was fabricated.

by PDCBI. The action spectra of the device clearly demonstrated that both TPD and PDCBI absorption contributed to the photovoltaic effect, as predicted from the energy level alignment.

The action spectrum also revealed that the response of device ITO/PEDOT/PAE-2:TPD:PDCBI/Al is very weak in the range of 380–450 nm, because there is little absorption due to either TPD or PDCBI. This can be improved by employing the concept of light harvesting, where a dye is used that can

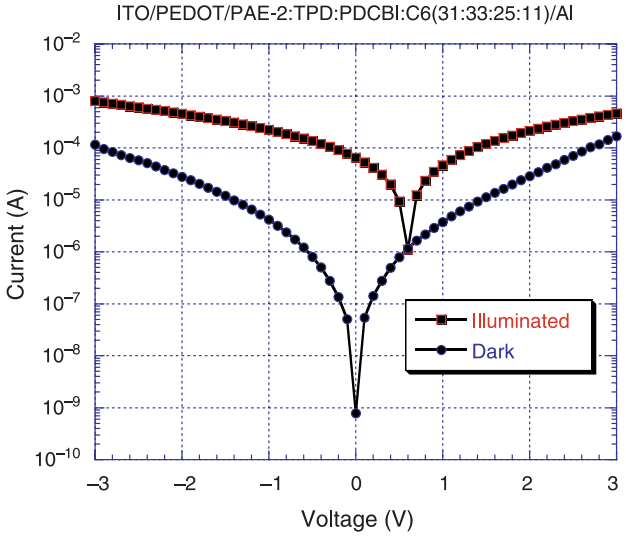

Fig. 4. *I–V* characteristics of ITO/PEDOT/PAE-2:TPD:PDCBI:C6 (31:33:25:11)/Al device in the dark and under illumination.

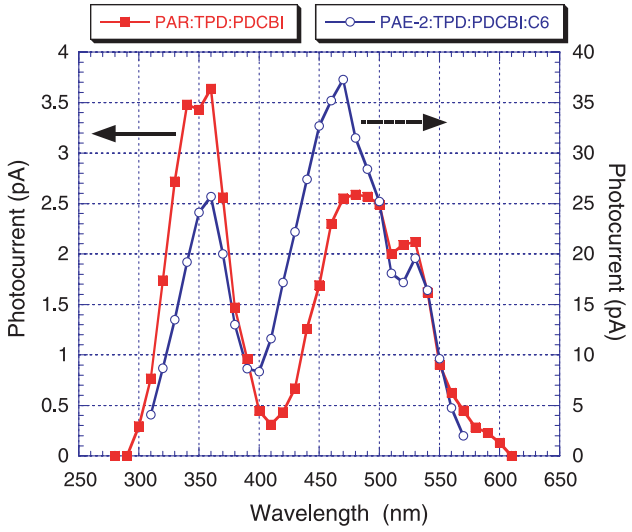

Fig. 5. Action spectra of ITO/PAR:TPD:PDCBI (37:30:34)/Al and ITO/PAE-2:TPD:PDCBI:C6 (31:33:25:11)/Al.

absorb in the range and then transfer the absorbed energy to PDCBI. Coumarin 6 (C6) is such a dye because the photoluminescence of C6 (spectrum not shown) overlaps well with the absorption spectrum of PDCBI. To demonstrate the concept, C6 was either blended in the photoactive layer, or used as a separate layer outside the device (on the opposite side of the glass substrate). The latter approach can avoid the penalty of resistance caused by the low charge mobility of C6, therefore providing a better photocurrent. The results are listed in Table 2. The action spectrum of the device with C6 in the photoactive layer is also shown in Fig. 5. Compared with the action spectrum of the device without C6, the response in the range of 400–500 is enhanced. The action spectrum also resembled the UV–vis absorption spectrum of PAE-2:TPD:PDCBI:C6 (31:33:25:11) blend film, which is shown in Fig. 6. This suggests the effectiveness of using C6 as the light harvesting material. From the energy level alignment, direct charge separation at C6/PDCBI interface followed by the

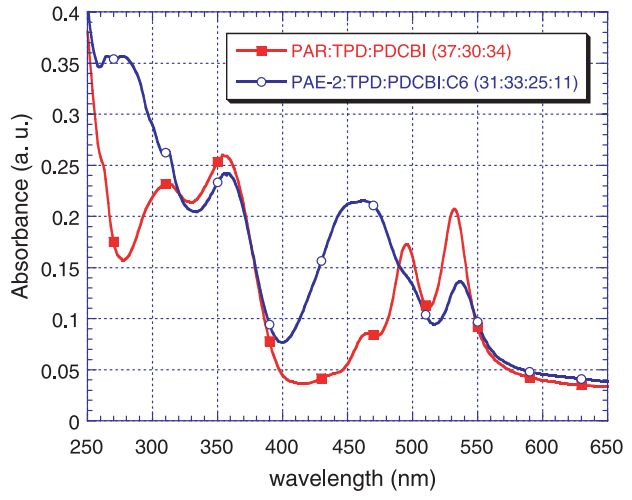

Fig. 6. UV–vis spectrum of PAR:TPD:PDCBI (37:30:34) and PAE-2:TPD:PDCBI:C6 (31:33:25:11) films on quartz substrate.

Table 3
Annealing effect on the performance of PV devices

Annealing protocol	Open circuit voltage (V)	Short circuit current (μA)	Fill factor
70 °C for 30 min	0.40	23.3	0.27
100 °C for 30 min	0.30	37.8	0.26
130 °C for 20 min	0.40	48.2	0.26
160 °C for 10 min	0.60	83.0	0.26

The device structure is ITO/PEDOT/PAE-2:TPD:PDCBI (31:40:29)/Ca (25 nm)/Ag (130 nm).

transport of holes to TPD might also contribute to the enhanced device performance.

The effect of annealing on the performance of PV devices was also studied. Table 3 summarizes the results. The short circuit currents are 23.3, 37.8, 48.2 and 83.0 μA after 70 °C (30 min), 100 °C (30 min), 130 °C (20 min) and 160 °C (10 min) annealing. It is obvious that annealing increases the short circuit current, probably due to improved morphology yielding a co-continuous structure (percolation network) and enhanced mobility resulting from the annealing treatment.

Since the absorption of TPD used as the hole transporting material in the PV devices fabricated is not ideal for solar cell applications, more hole transporting materials were tested, including 2,7,12,17-tetra-*tert*-butyl-5,10,15,20-tetraaza-21H,23H-porphine(TBPP), 2,3,7,8,12,13,17,18-octaethyl-21H,23H-porphine zinc(II) (ZnOEP), and 2,3,7,8,12,13,17,18-octaethyl-21H,23H-porphine magnesium(II) (MgOEP). PAR was used as the matrix and PDCBI as electron transporting material. Table 4 summarizes the performance of the PV devices. The fill factor of the devices is also relatively low, probably due to the high resistance of the photoactive layer. Typical *I–V* curves of the device ITO/PEDOT/PAR:MgOEP:PDCBI (50:22:28)/Al, both in the dark and under illumination, are shown in Fig. 7.

One potential advantage of using the large ring porphyrin molecules is that the triplet state of these molecules has a longer lifetime (e.g. the triplet lifetime of ZnOEP is in the range of millisecond) and can diffuse through a longer distance than a singlet exciton. As a result, the triplet exciton has a higher probability to reach an interface where charge separation can occur. Compared with other devices, the loading ratio of ZnOEP and PDCBI in this experiment is lower. A high loading ratio will probably generate better performance.

Table 4
Performance of PV devices with structure of ITO/PEDOT/photoactive layer/cathode

Sample	Active layer	Open circuit voltage (V)	Short circuit current (A)	Fill factor
19057-18-2	PAR:TBPP:PDCBI (56:25:19)	0.10	2.66×10^{-9}	0.26
19057-18-3	PAR:ZnOEP:PDCBI (63:18:19)	0.60	1.14×10^{-6}	0.28
19057-18-4	PAR:MgOEP:PDCBI (50:22:28)	0.40	1.77×10^{-6}	0.28

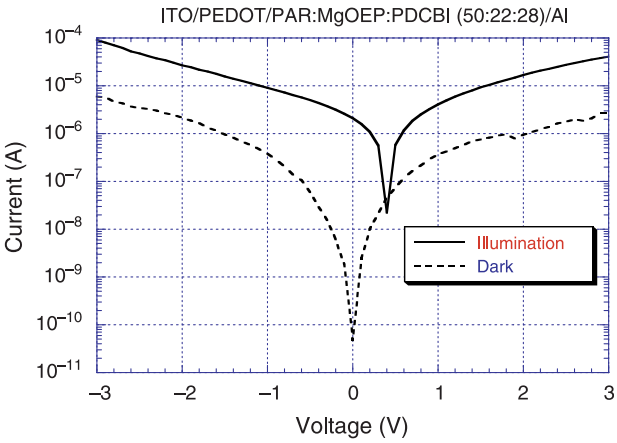

Fig. 7. Representative *I–V* curves for the ITO/PEDOT/PAR:MgOEP:PDCBI (50:22:28)/Al device in the dark and under illumination.

In PV devices that use high T_g polymer matrix to sequester the electroactive (hole or electron transporting) small molecules, two or more high T_g polymers can be used together. To demonstrate this concept, two PV devices were fabricated with structures of ITO/PEDOT/PAR:PAE-2:TPD:PBCDI (24:24:27:25) (90 nm)/Al and ITO/PEDOT/-PAR:MEH-PPV:TPD:PBCDI (16:19:31:34) (~60 nm)/Al. A V_{oc} of 0.6 V and an I_{sc} of 12.7 μA were measured from the first device with PAR and PAE-2 as the matrix material. A V_{oc} of 0.5 V and an I_{sc} of 40.1 μA were measured from the second device with PAR and MEH-PPV as the matrix. When the polymers are properly selected, the two polymers could be phase separated and preferentially bind one small molecule into each phase, providing a better continued transport pathway for holes and electrons transport in the corresponding phase.

4. Conclusions

Previous approaches in LED and PV devices to solve the basic problems of low molecular weight electroactive species (low T_g, crystallization, poor mechanical properties, limited ability to employ lower cost fabrication routes) have often involved covalent bonding of these species to polymeric backbones. This study investigated a simpler blend approach. The use of high T_g polymers to sequester low molecular weight electroactive compounds in the light harvesting layer of PV devices has been demonstrated. Combinations of hole transport and electron transport (electron donor–electron acceptor) pairs optionally combined with light harvesting materials (e.g. laser dyes) yields open circuit voltage and short circuit currents in the range of more conventional organic/polymer based PV devices. Fill factors are low presumably due to higher than desired resistances of the photoactive layer. The use of the high T_g polymer allows for the use of low molecular weight electroactive materials in easier, lower cost fabrication routes. The addition of the higher T_g polymer also allows for improved mechanical properties of the active layer of the PV device of

potential interest for flexible PV devices. The results reported in this study are not optimized; and with the many variables involved with this concept, significant improvements should be possible.

References

[1] Gay CF. 4th eds Encyclopedia of chemical technology, vol. 18. New York: Wiley; 1996 p. 964–91.
[2] Kuwano Y. 5th eds Ulmanns's encyclopedia of industrial chemistry, vol. A20. Weinheim, Germany: VCH Publishers; 1992 p. 161–80.
[3] Ghosh AK, Morel DL, Feng T, Shaw RF, Rowe Jr CA. J Appl Phys 1974; 45:230–6.
[4] Gamblin RL. IBM Tech Discuss Bull 1976;18:2442.
[5] Tang CW. Appl Phys Lett 1986;48:183–5.
[6] Kaneko M, Yamada A, Kenmochi T, Tsuchida E. J Polym Sci, Polym Lett Ed 1985;23:629–31.
[7] Yu G, Gao J, Hummelen JC, Wudl F, Heeger AJ. Science 1995;270: 1789–91.
[8] Yu G, Heeger AJ. J Appl Phys 1995;78:4510–15.
[9] Arias AC, MacKenzie JD, Stevenson R, Halls JJM, Inbasekaran M, Woo EP, et al. Macromolecules 2001;34:6005–13.
[10] Peumans P, Uchida S, Forrest SR. Nature 2003;425:158–62.
[11] Nelson J. Curr Opin Solid State Mater Sci 2002;6:87–95.
[12] Brabec CJ, Sariciftci NS, Hummelen JC. Adv Funct Mat 2001;11:15–26.
[13] Yang MJ, Lu SL, Li Y. J Mater Sci Lett 2003;22:813–5.
[14] Kim HS, Kim CH, Ha CS, Lee JK. Synth Met 2001;117:289–91.
[15] Jain SC, Aernout T, Kapoor AK, Kumar V, Geens W, Poortmans J, et al. Synth Met 2005;148:245–50.
[16] Roder T, Kitzerow HS, Hummelen JC. Synth Met 2004;141:271–5.
[17] Lee JH, Seoul C, Park JH, Youk JH. Synth Met 2004;145:11–14.
[18] McNeill CR, Frohne H, Holdsworth JL, Dastoor PC. Synth Met 2004;147: 101.
[19] Tang CW, Marchetti AP, Young RH. US 4,125,414; 1978.
[20] Loutfy RO, McIntyre LF, Sharp JH. US 4,175,981; 1979.
[21] Stolka M, Pai DM, Yanus JF. US 4,115,116; 1978.
[22] Limburg WW, Pai DM, Pearson JM, Renfer D, Stolka M, Turner R, et al. Org Coat Plast Chem 1978;38:534–9.
[23] Minami N, Sasaki K, Tsuda K. J Appl Phys 1983;54:6764–6.
[24] El-Shaarawy MG, Mansour AF, El-Bashir SM, El-Mansy MK, Hammam M. J Appl Polym Sci 2003;88:793–805.
[25] Marin V, Holder E, Wienk MM, Tekin E, Kozodaev D, Schubert US. Macromol Rapid Commun 2005;26:319–24.
[26] Robeson LM, Jiang XZ, Burgoyne Jr WF. ANTEC 2004, the annual technical conference sponsored by society of plastics engineers, May 16–20, Chicago, IL; 2004. p. 2284–8.
[27] Robeson LM, Jiang XZ, Burgoyne, Jr WF. US Pat Appl 2005/0022865; 2005.
[28] Burgoyne, Jr WF, Robeson LM, Vrtis RN. US 5,874,516; 1999.
[29] Robeson LM, Maresca LM. In: Margolis JM, editor. Engineering thermoplastics: properties and applications. New York: Marcel Dekker; 1985. p. 225–81.
[30] Mello JC, Wittmann HF, Friend RH. Adv Mater 1997;9:230–2.
[31] Ruhstaller B, Carter SA, Barth S, Riel H, Riess W, Scott JC. J Appl Phys 2001;89:4575–86.
[32] Qiu CF, Wang LD, Chen HY, Wong M, Kwok HS. Appl Phys Lett 2001; 79:2276–8.
[33] Greenwald Y, Xu X, Fourmigue M, Srdanov G, Koss C, Wudl F, Heeger AJ. J Polym Sci, Part A: Polym Chem 1998;36:3115–20.
[34] Hill IG, Schwartz J, Kahn A. Org Electron 2000;1:5–13.